Iranian Polymer Journal
18 (2), 2009, 167-178

Available online at: http://journal.ippi.ac.ir

Study of Non-isothermal Crystallization Kinetics of Single-walled Carbon Nanotubes Filled Polypropylene Using Avrami and Mo Models

Mohammad Razavi-Nouri

Iran Polymer and Petrochemical Institute, P.O.Box:14965-115, Tehran, Iran

Received 6 September 2008; accepted 12 January 2009

ABSTRACT

The kinetics of non-isothermal crystallizations of polypropylene (PP) and PP containing 0.5 wt% single-walled carbon nanotube (PP/SWNT) were compared by using differential scanning calorimetry technique. The non-isothermal melt crystallization data were analyzed according to Avrami and Mo models. The values of half-life and corrected composite rate constant of Avrami equation as well as the rate parameter of Mo equation indicated that the crystallization rate increased with the increasing of PP and PP/SWNT cooling rates. However, the crystallization rate of the nanocomposite was found to be higher than that of PP at a certain cooling rate. Nucleation efficiency (NE) defined by Fillon was obtained for PP/SWNT. It was found that NE varied from 16.4% to 19.4% in the range of cooling rate studied. This implied that SWNT could play as a nucleating agent for the crystallization of PP. In addition, the effective energy barrier (ΔE) for the non-isothermal melt crystallization process was calculated for the two materials by using the Kissinger method. The ΔE values were determined to be 226 and 262 $kJmol^{-1}$ for PP and PP/SWNT, respectively. Based on the theory proposed by Lauritzen and Hoffman, the end surface free energy (σ_e) for the two materials was calculated. The results showed that the value of σ_e for the nanocomposite was lower than that of PP itself, in agreement with the fact that the rate of crystallization is higher in the nanocomposite compared to the pristine polymer.

Key Words:

polypropylene;
carbon nanotube;
non-isothermal crystallization kinetics;
nucleation efficiency;
kinetic crystallizability.

(*) To whom correspondence to be addressed.
E-mail: m.razavi@ippi.ac.ir

INTRODUCTION

Carbon nanotubes (CNTs) have received immense attentions and have been the subject of investigation by scientific communities around the world for the past few years [1-10]. Due to strong carbon-carbon bonds and more or less perfect crystalline structure, CNTs are among the materials with outstanding physical and mechanical properties. They can be produced in two different forms of single-walled (SWNT) and multi-walled (MWNT) structures which in the former the nanotube wall consists of only one layer of carbon atoms and the latter is made of several concentric cylinders around a central hollow [11-13]. The high stiffness, strength, and conductivity of CNTs as well as their high aspect ratio and large surface area have led interests towards carbon nanotube-reinforced polymers (CNTRP) as ultra light structural polymers with superb mechanical properties [14-21].

Studies on the kinetics of poly-

mer crystallization are theoretically and practically important. Because of simplicity in interpretation and fitting the data with the existed theories most of the experiments are conducted in isothermal conditions. However, in practice, polymers are usually produced and processed in non-isothermal conditions such as injection moulding or extrusion. As the physical and mechanical properties of polymers are strongly dependent on morphology and the extent of the crystallinity formed during such processing conditions, it is very important to extend our knowledge on the non-isothermal crystallization kinetics of polymer materials [22].

There are a few published papers about the non-isothermal crystallization kinetics of polypropylene/CNT nanocomposites, however, most of them have been focused on the kinetics of isothermal crystallization [23-26] and in some of them non-isothermal crystallization kinetics was also examined for the materials crystallized under just one cooling rate [26,27]. In these papers the analysis was carried out using only Avrami equation, except Leelapornpisit et al. [28] who used Mo model to analyze the non-isothermal crystallization of the materials.

In this paper, a comprehensive study has been made on the non-isothermal crystallization kinetics of polypropylene and the one containing single-walled carbon nanotubes (SWNTs). The Avrami and Mo models are applied to deal with the experimental data obtained using the differential scanning calorimetry (DSC) technique. The activation energies for non-isothermal crystallization process have been calculated for the two materials according to the Kissinger proposed equation. At the end, the kinetic crystallizability has been calculated for the two materials by a method proposed by Jeziorny and also the kinetics of non-isothermal crystallization has also been analyzed using the equation proposed by Lauritzen and Hoffman. To the best of our knowledge nobody has yet reported the two latter models to study the non-isothermal kinetics of polymer filled CNT nanocomposites.

EXPERIMENTAL

Materials

PP homopolymer was supplied by Bandar Imam Petrochemical Co., Iran, as the grade Poliran PI0800. The melt flow index and density were 8 g/10 min and 0.902 g/cm^3, respectively. The SWNTs were obtained from Research Institute of Petroleum Industry (RIPI), Iran, with the maximum length of 10 μm. It was prepared by using a chemical vapour deposition (CVD) process via methane as a carbon source, cobalt and molybdenum as a catalyst system and reaction temperature range 800-1000ºC.

Composite Preparation

SWNTs were dried under vacuum at 80ºC for 12 h to remove any moisture before mixing with other ingredients. The mixing of the components was performed in an internal mixer (Haake Rheomix; HBI SYS90) with rotor speed of 120 rpm and at 180°C. PP granules and SWNTs (0.5 wt%) were all dry blended first and then introduced into the mixer and mixing continued for 10 min. The mixture was compression moulded after mixing was finished. Square plaque (0.5 mm thick) of the mixture was prepared in a Toyoseiki Mini Test Hydraulic Press (Japan) at 190°C and 10 MPa for 5 min. Then the sheets were directly quenched in water at room temperature.

Thermal Analysis

Thermal analysis was carried out using a Perkin-Elmer DSC (model Pyris I) interfaced to a personal computer. The temperature scale of the calorimeter was calibrated by indium. All samples were weighed (5±0.2 mg) and each sample was enclosed in an aluminium pan. An empty aluminium pan was also used as a reference. The samples were first heated to 210ºC and to ensure complete melting, the samples were kept at this temperature for 5 min. After this period, each sample was cooled to 50ºC at the cooling rates of 2.5, 5, 10, 20, and 40 K.min^{-1}. The non-isothermal crystallization exotherms were recorded for further analysis.

RESULTS AND DISCUSSION

Crystallization Behaviour of PP and PP/SWNT

The crystallization exotherms of PP and PP containing 0.5 wt% of SWNTs (PP/SWNT) for non-iosthermal crystallization from the melt at different cooling

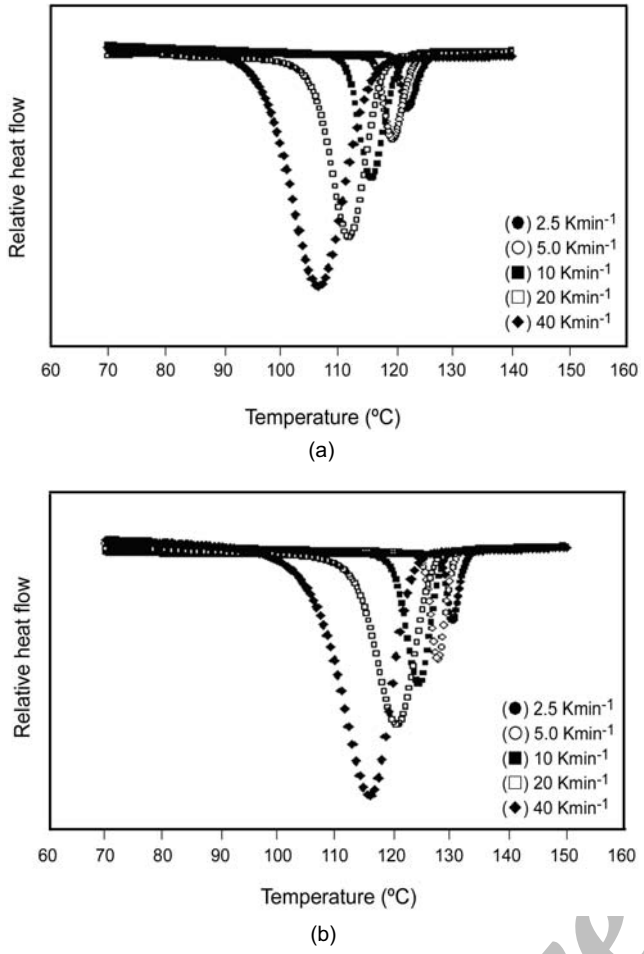

Figure 1. DSC non-isothermal crystallization curves of: (a) PP and (b) PP/SWNT.

rates are shown in Figures 1a and 1b, respectively. It is obvious that the exothermic trace has become wider and the peak temperature (T_p) shifted to lower temperature for PP and PP/SWNT when the cooling rate increased. When the cooling rate is low, the molecular chains of PP have sufficient time to overcome the nucleation energy barrier and consequently make a more perfect crystal and show a higher T_p [29].

It can also be seen that at the same cooling rate the T_p of PP/SWNT nanocomposite is higher than that of the pristine polymer (Figure 2). This can be related to the heterogeneous nucleation effect of the SWNTs on PP chain segments crystallization. Aggregates and the solid surfaces of SWNTs and also the other impurities can serve as nuclei on which the PP chains can easily be absorbed and lead to PP crystallization more quickly at higher temperature.

Nucleation efficiency (NE) for a given polymer

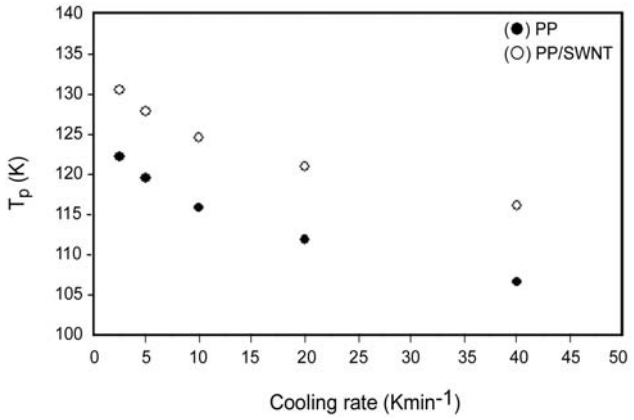

Figure 2. Variation of peak crystallization temperature versus cooling rate for PP and PP/SWNT.

has been defined by Fillon et al. as follows [30]:

$$NE = \frac{T_{CNA} - T_{C1}}{T_{C2\,max} - T_{C1}} \times 100 \qquad (1)$$

where T_{C1} is the crystallization temperature of polymer without any nucleating agent, T_{CNA} is the peak crystallization temperature of polymer containing nucleating agent and T_{C2max} is the optimum self-nucleation temperature which has been reported to be 164.5ºC for PP [29]. According to the two extreme cooling rates of 2.5 and 40 K.min^{-1}, the calculated NE for PP/SWNT was between 19.4% and 16.4%. This implies that SWNTs can play the role of nucleating agent in PP.

Non-isothermal Crystallization Kinetics

Modified Avrami Analysis

Avrami equation which is widely used to analyze the isothermal crystallization of polymers is expressed as follows [31-34]:

$$-ln(1 - X_t) = Zt^n \qquad (2)$$

where Z is the composite rate constant incorporating both nucleation and growth, X_t is the relative degree of crystallinity and n is the Avrami exponent which depends on nucleation mechanism and growth dimension [35]. Using eqn (2) in double-logarithm form, eqn (3) may be written as follows:

$$log(-ln(1 - X_t)) = log\, Z + n \log t \qquad (3)$$

By plotting log(-ln(1-X_t)) against log t for each cooling rate, the two adjustable parameters of Z and n can be obtained. X_t, as a function of time, can be calculated using the following equation [36-38]:

$$X_t = \frac{\int_{t_0}^{t} \frac{dH}{dt} dt}{\int_{t_0}^{t_\infty} \frac{dH}{dt} dt} \quad (4)$$

where t_0 and t_∞ are the starting and the ending times of crystallization, respectively and dH/dt is the rate of heat evolution. The modified form of Avrami equation can be used for analyzing non-isothermal crystallization. In this case X_t is a function of crystallization temperature and is defined as follows [39]:

$$X_t = \frac{\int_{T_0}^{T} \frac{dH}{dT} dT}{\int_{T_0}^{T_\infty} \frac{dH}{dT} dT} \quad (5)$$

where T_0 and T_∞ indicate the crystallization temperatures at the starting and ending points, respectively.

According to Jeziorny [40] at a constant cooling rate Z should be corrected using the cooling rate employed during non-isothermal crystallization experiment as follows:

$$\log Z_C = \frac{\log Z}{\varphi} \quad (6)$$

where Z_c is the corrected composite rate constant and φ = dT/dt is the cooling rate.

The relation between crystallization time and temperature during the non-isothermal crystallization process is given by:

$$t = \frac{|T_0 - T|}{\varphi} \quad (7)$$

where T is the temperature at time t [39].

The variations of X_t as a function of temperature for PP and PP/SWNT at various cooling rates are presented in Figures 3a and 3b, respectively. All the curves show the same inversed sigmoidal shape,

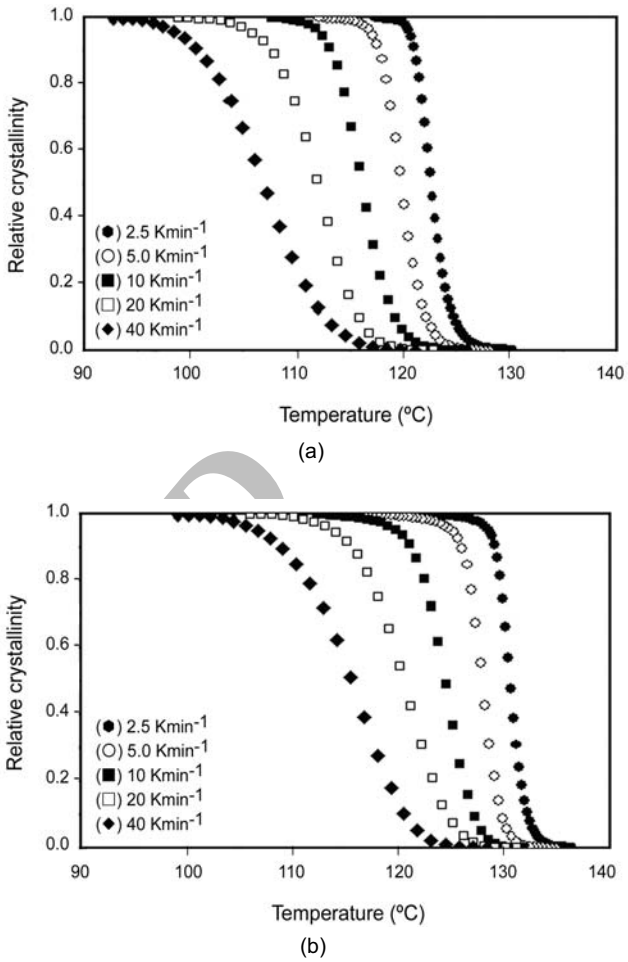

Figure 3. Relative crystallinity against the crystallization temperature at various cooling rates for: (a) PP and (b) PP/SWNT.

signifying that the shifts observed are only related to the delay effect of cooling rate on crystallization [41].

Figures 4a and 4b can be plotted if the temperature scale is converted into a time scale using eqn (7). It is clearly observed that the time which is required for the completion of crystallization decreased as the cooling rate increased. It is also quite clear that at a given cooling rate, the crystallization time of PP/SWNT is shorter than that of the PP itself.

Figures 5a and 5b show the plots of log(-ln(1-X_t)) against log t for PP and PP/SWNT at different cooling rates. Each curve consists of two parts with different slopes in which the first part with larger slope is related to primary crystallization process and the second part with smaller slope is attributed to the secondary crystallization process [42]. It is note-

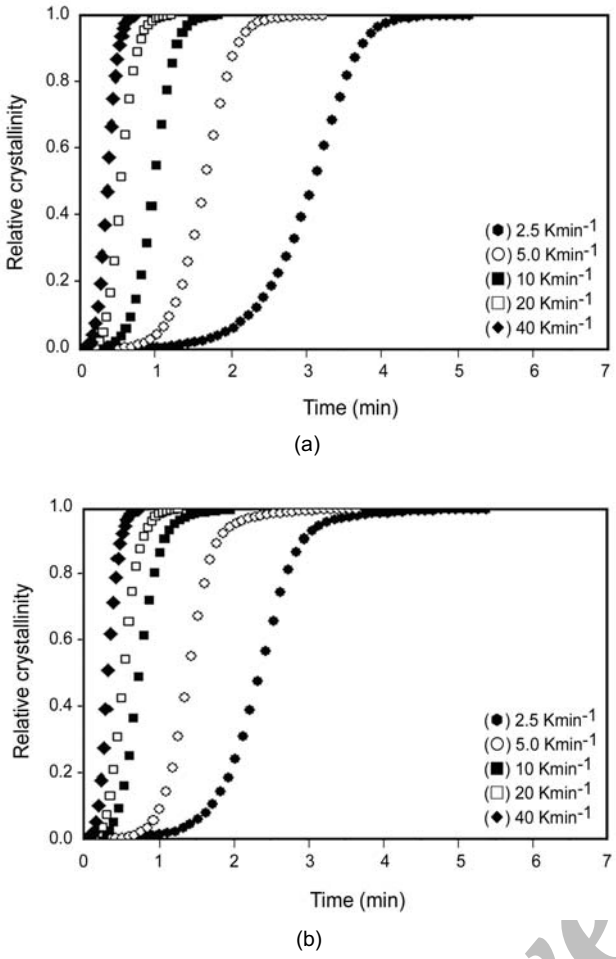

Figure 4. Relative crystallinity against crystallization time at various cooling rates for: (a) PP and (b) PP/SWNT.

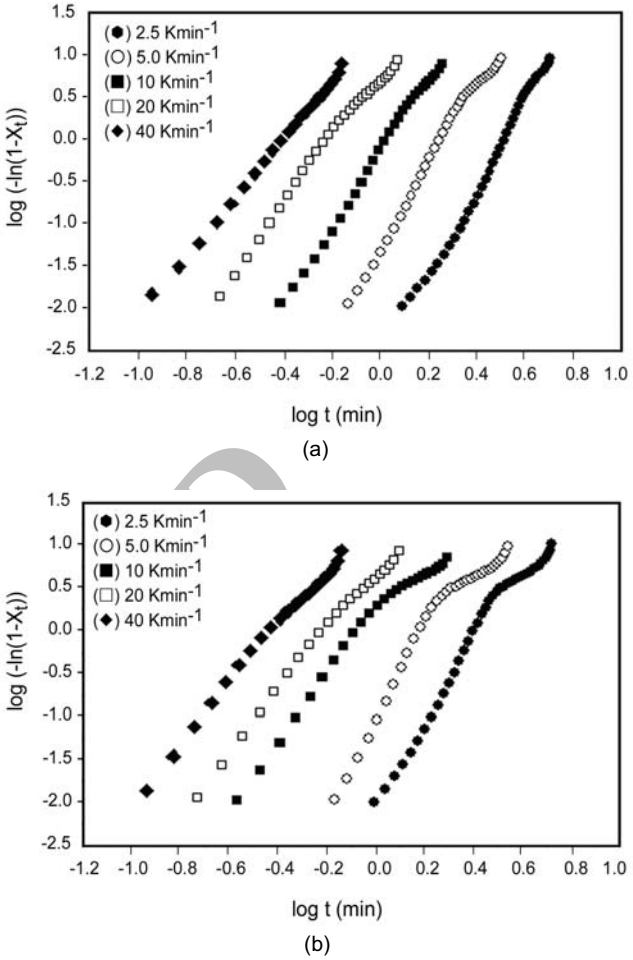

Figure 5. Plots of log(-ln(1-X_t)) against log t for crystallization of: (a) PP and (b) PP/SWNT.

worthy that in non-isothermal crystallization Z and n cannot have the same physical significance as they have in isothermal crystallization [29,41,43] and the values of n show more divergence for the former than the values obtained for the latter [41,44]. This is because the temperature in non-isothermal crystallization condition changes continuously and it has a serious effect on the rates of spherulite growth and nucleation which are both temperature dependent. Thus, from the first linear part of the plot, the values of parameters of crystallization half-life ($t_{1/2}$), n and Z were determined at different cooling rates.

The results obtained from the Avrami plots and the Jeziorny method are tabulated in Table 1. It can be seen that the relative degree of crystallinity formed at the end of primary crystallization process ($X_{P,\infty}$) shifts to the lower values for the two materials as the cooling rate increases. However, the amount of shift is more pronounced for the PP/SWNT, implying that secondary crystallization process is more significant for PP/SWNT than that of PP itself.

The Avrami exponent varied from 3.70 to 5.48 for PP and from 4.19 to 6.13 for PP/SWNT. As it can be seen, $t_{1/2}$ value decreases and Z value increases with increasing cooling rate indicating that the polymer has crystallized faster when the cooling rate is increased. However, at the same cooling rate, for PP/SWNT the value of $t_{1/2}$ is lower and the value of Z is higher compared to these values of the pristine polymer. Z_c is also increased with cooling rate as expected and it is higher in values for the nanocomposite in comparison with PP alone. These are consistent with the fact that the crystallization rate of PP/SWNT is higher than that of the pristine polymer.

Table 1. Non-isothermal crystallization kinetics parameters of PP and PP/SWNT nanocomposite at different cooling rates.

Sample	φ (Kmin^{-1})	$t_{1/2}$ (min)	n	Z (×10^3) (min^{-n})	Z_c	$X_{P,\infty}$
PP	2.5	3.07	5.12	2.25	0.087	0.97
	5	1.63	5.48	48	0.545	0.94
	10	0.96	4.79	860	0.985	0.92
	20	0.50	4.56	16539	1.151	0.85
	40	0.32	3.70	47998	1.096	0.80
PP/SWNT	2.5	2.31	5.27	8.32	0.147	0.92
	5	1.35	6.13	110	0.643	0.87
	10	0.70	4.36	3245	1.125	0.85
	20	0.46	4.18	16442	1.150	0.72
	40	0.27	4.19	177272	1.138	0.62

Mo Model Analysis

Assuming that non-isothermal crystallization process can be composed of infinitesimally small isothermal crystallization steps, Ozawa [45] modified the Avrami equation by taking into account the effect of cooling rate on the crystallization process from the melt to the glassy state. He replaced t in eqn (2) with T/φ as follows:

$$1 - X_t = exp[\frac{-K(T)}{\varphi^m}] \quad (8)$$

or

$$log[-ln(1 - X_t)] = log\, K(T) - m\, log\, \varphi \quad (9)$$

where m is the Ozawa exponent that depends on the dimension of the crystal growth and K(T) is defined as a cooling function.

Mo et al. [46,47] proposed another model for non-isothermal crystallization based on Avrami and Ozawa equations. For the same system, at a certain degree of crystallinity and crystallization time, the right hand sides of eqns (3) and (9) should be equal. Therefore, a new equation is obtained for non-isothermal crystallization such as:

$$log\, Z + n\, log\, t = log\, K(T) - m\, log\, \varphi \quad (10)$$

By rearranging the equation we have:

$$log\, \varphi = log\, F(T) - \alpha\, log\, t \quad (11)$$

where α = n/m, the ratio of Avrami to Ozawa exponent, and F(T) = [K(T)/Z]$^{1/m}$. F(T) indicates the value of cooling rate which has to be chosen at unit crystallization time when the measured system amounts to a certain degree of crystallinity. According to eqn (11) a straight line is obtained by plotting log φ against log t for a certain relative degree of crystallinity.

Figures 6a and 6b show the analysis for PP and PP/SWNT, respectively, at several X_t values of 20%, 40%, 60% and 80%. It can be seen that the plots produce a series of straight lines for the two materials at a given X_t. This clearly shows that the Mo method is successful in describing the non-isothermal process of PP and PP/SWNT. The values of α can be calculated from the slope and that of F(T) from the intercept of the lines.

The values of α and F(T) calculated for the two materials are listed in Table 2. The value of α varies from 1.20 to 1.34 for PP and from 1.29 to 1.50 for PP/SWNT. It is observed that the value of F(T) systematically increases with X_t but at the same X_t value, PP reveals a higher F(T) value comparing to the value obtained for PP/SWNT. Since F(T) reflects the difficulty of crystallization process [34] the smaller values determined for PP/SWNT is in agreement with faster crystallization rate of nanocomposite compared to that of the PP itself. This is consistent with Avrami

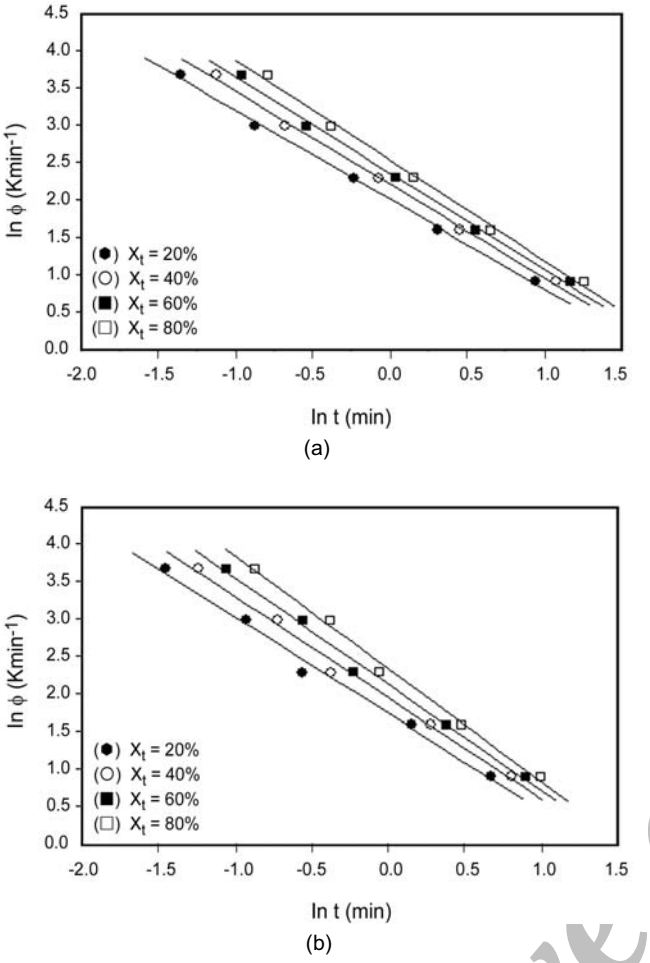

Figure 6. Plots of ln φ as a function of ln t at several relative crystallinities for: (a) PP and (b) PP/SWNT.

analysis results and also with our previous observation that SWNTs act as nucleating agents.

The Kinetic Crystallizability

Based on Ziabicki's theory [48], Jeziorny [40] derived an equation to calculate a parameter known as the kinetic crystallizability, G, in order to characterize the non-isothermal crystallization kinetics of poly(ethylene terephthalate). The expression of this parameter is given as follows:

$$G = \left(\frac{\pi}{\ln 2}\right)^{0.5} K_{max}\frac{D}{2} \approx 1.064\frac{\int_{t_0}^{t_{max}}\frac{dH}{dt}dt}{\int_{t_{max}}^{t_f}\frac{dH}{dt}dt}\frac{D}{t_{max}} \qquad (12)$$

where D is the half-width of the crystallization peak

Table 2. Non-isothermal crystallization kinetics parameters of PP and PP/SWNT nanocomposite at different relative crystallinities.

Sample	X_t (%)	α	F(T)
PP	20	1.20	7.48
	40	1.25	9.14
	60	1.29	10.67
	80	1.34	12.69
PP/SWNT	20	1.29	5.78
	40	1.35	7.15
	60	1.42	8.53
	80	1.50	10.53

and K_{max} is the ratio of relative crystallinity from the time that crystallization begins, t_0, up to the time corresponding to maximum crystallization rate, t_{max}, and from the latter to the point that crystallization ends, t_f, divided by t_{max}. The kinetic crystallizability characterizes the degree of crystallinity obtained when a polymer is cooled from its melting temperature to its glass transition temperature at unit cooling rate [49]. Therefore, G similar to Z should be corrected by considering the influence of φ as follows:

$$G_C = \frac{G}{\varphi} \qquad (13)$$

The parameters characterizing the non-isothermal kinetic crystallizabilities of PP and the nanocomposite are listed in Table 3. The results show that the value of G_c is not dependent on cooling rate for the two materials at all cooling rates studied. The average G_c values of 1.247 for PP and 1.158 for the nanocomposite also reveal that this parameter is not influenced much by the presence of CNTs in PP.

Activation Energy of Crystallization

The Kissinger method can often be used to estimate the activation energy in various cooling rates [50];

$$\frac{d\left(ln\left(\frac{\varphi}{T_P^{\,2}}\right)\right)}{d\left(\frac{1}{T_P}\right)} = \frac{-\Delta E}{R} \qquad (14)$$

where ΔE is the activation energy of crystallization

Table 3. Kinetic crystallizability of PP and PP/SWNT at different cooling rates.

Sample	φ (Kmin^{-1})	D (K)	K_{max} (min^{-1})	G (Kmin^{-1})	G_c
PP	2.5	3.022	1.008	3.243	1.297
	5	3.702	1.566	6.171	1.234
	10	4.927	2.308	12.105	1.210
	20	6.920	3.392	24.986	1.249
	40	10.531	4.448	49.862	1.247
PP/SWNT	2.5	2.351	1.096	2.743	1.097
	5	2.905	1.793	5.544	1.109
	10	4.764	2.299	11.659	1.166
	20	7.606	3.136	25.390	1.270
	40	9.763	4.409	45.820	1.146

and R is the universal gas constant.

Figure 7 shows the plots of $\ln(\varphi/T_p^2)$ against $1/T_p$ from which the activation energy of non-isothermal melt crystallizations of PP and PP/SWNT were detemined from the slope of each line. The ΔE value was calculated to be 226 and 262 kJmol^{-1} for PP and PP/SWNT, respectively. It is observed that the addition of SWNTs unexpectedly increased the ΔE value. This phenomenon has also been reported for PP nucleated with sodium benzoate [51], rosin-based nucleating agents [52], and even poly(trimethylene terephthalate) (PTT)/clay [53] and polyethylene (PE)/clay nanocomposites [29]. The higher ΔE for PP/SWNT reveals that the introducing of SWNTs to PP makes the transportation of PP chains segments to the growing crystal surface more difficult [54]. However, apart from the higher activation energy obtained for PP/SWNT, the other kinetics data such as $t_{1/2}$ and Z (and Z_c) clearly showed that the addition of SWNTs could enhance the rate of PP crystallization.

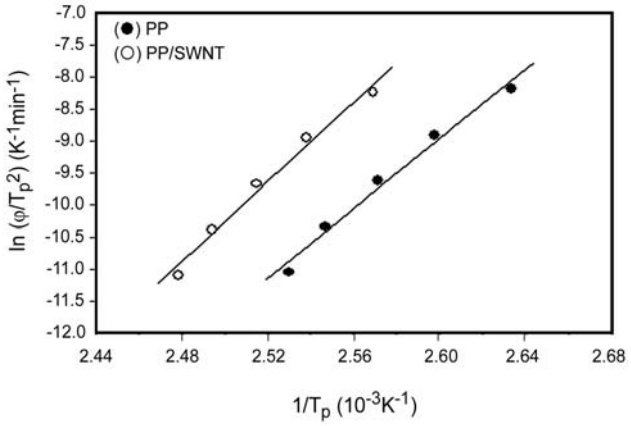

Figure 7. Plots of $\ln(\varphi/T_p^2)$ against $1/T_p$ for PP and PP/SWNT.

It has been proposed for polymer/clay nanocomposites that because of the existence of pre-existed silicate staking nuclei, the chains which are located in the neighbourhood of the stakes may aggregate instead of folding through a reptation tube in the presence of clay. It means that the rate of aggregation of chains, close to nanoclay is much higher than that of chain folding [55]. In the case of PP/SWNT, it has been suggested that the increase of PP viscosity after SWNTs introduction depresses the rearrangement of PP molecular chains [28]. Thus, the value of activation energy is higher for the nanocomposite than that of PP.

Analysis of Crystallization Kinetics According to Lauritzen-Hoffman Expression

Based on the Turnbull and Fisher equation [56], Hoffman et al. proposed an expression for the analyzing of the temperature dependence linear growth rate [57-61] as follows:

$$g = g_0 \exp\left(\frac{-\Delta E}{R(T_C - T_\infty)}\right) \exp\left(\frac{-K_g}{fT_C \Delta T}\right) \qquad (15)$$

where g is the growth rate, g_0 is a temperature inde-

pendent pre-exponential parameter, ΔE is the energy barrier for transport of material across the crystal-liquid interface, T_∞ is the temperature below which motions cease and is taken as $T_\infty = T_g - 30K$, R is the universal gas constant, f which is obtained from $f = 2T_c/(T_m^0+T_c)$ expression is a correction factor that accounts for the change of the enthalpy of fusion, ΔH_f, with temperature, T_c is crystallization temperature and $\Delta T = T_m^0 - T_c$ is the degree of undercooling in which T_m^0 is the equilibrium melting temperature, and K_g is the nucleation constant which is expressed as follows:

$$K_g = \frac{nb_0\sigma\sigma_e T_m^0}{k\Delta H_f} \quad (16)$$

where n is a parameter which depends on the crystallization regime according to Lauritzen-Hoffman theory, σ and σ_e are the lateral and end surface free energies of the growing crystal, respectively, b_0 is the molecular thickness, and k is the Boltzmann constant. σ can also be estimated as follows:

$$\sigma = \alpha(a_0 b_0)^{0.5}\Delta H_f \quad (17)$$

where α was empirically obtained to be 0.1 and a_0b_0 represents the cross-sectional area of the polymer chain [62].

Assuming that the three-dimensional crystal growth has linear relationship with time, the overall kinetic parameter K which is considered to be equivalent to Z_c can be expressed as follows [63].

$$K = (\frac{4\pi}{3})g^3 N \quad (18)$$

where N is the nucleation density. The result of combining eqns (15) and (18) will be the following equation:

$$\frac{1}{3}\ln K + \frac{\Delta E}{R(T_C - T_\infty)} = A_0 - \frac{K_g}{fT_C\Delta T} \quad (19)$$

where, $A_0 = \ln g_0 + 1/3\ln 4\pi N/3$. The plots of $1/3\ln K + \Delta E/R(T_c-T_\infty)$ against $1/fT_c\Delta T$ for PP and PP/SWNT are shown in Figure 8. The values of K_g can directly be calculated from the slope of the lines. Therefore, the value of σ_e can simply be estimated by using eqns (16) and (17).

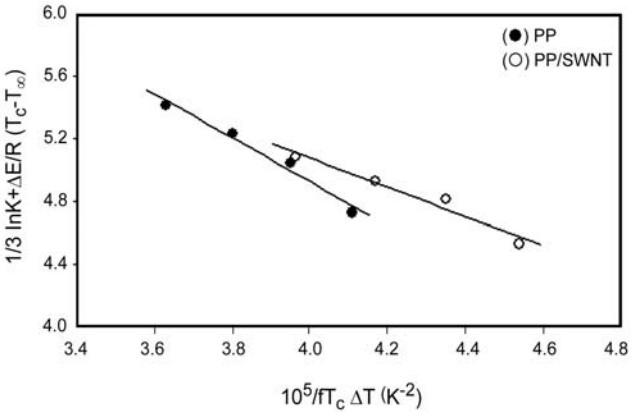

Figure 8. The plots of $1/3\ln K + \Delta E/R(T_c-T_\infty)$ against $1/fT_c\Delta T$ for PP and PP/SWNT nanocomposite.

In order to calculate the K_g and σ_e the values of a_0, b_0, T_g, ΔE and T_m^0 were taken to be 5.49×10^{-10} m, 6.26×10^{-10} m , 269.6 K, 6280 $Jmol^{-1}$ [64] and 460 K [65], respectively. The σ_e decreased from 29 mJ/m^2 for the pristine polymer to 19 mJ/m^2 for PP/SWNT nanocomposite. This means that the addition of SWNTs to PP depresses the chain folding barrier, thus, increases the rate of crystallization of PP [13,63,66]. This is consistent with what we have reported earlier.

CONCLUSION

The study of non-isothermal crystallization kinetics of PP and PP/SWNT was carried out by DSC. Calculation of nucleation efficiency showed that SWNTs could serve as nuclei and increase the heterogeneous nucleation in PP. The results obtained from Avrami analysis indicated that at the same cooling rate, PP/SWNT has lower value of $t_{1/2}$ and higher value of Z (and Z_c) compared to the pristine polymer. These were in agreement with faster crystallization rate of PP/SWNT than that of the PP itself. Mo method was found to be a suitable and convenient method to deal with the non-isothermal crystallization of PP and the nanocomposite. This method also proved that the faster crystallization of nanocomposite compared to PP is consistent with the results obtained by the Avrami analysis. The activation energy of melt crystallization for the PP and PP/SWNT

was determined to be 226 and 262 kJmol^{-1}, respectively. The unexpected higher amount of activation value for the nanocomposite could be attributed to the higher viscosity of the nanocomposite than to that of the pristine polymer. The reduction of σ_e in the nanocomposite compared to PP alone was also consistent with the higher rate of crystallization of PP in the nanocomposite.

REFERENCES

1. Valentini L, Biagiotti J, Kenny JM, López-Manchado MA, Physical and mechanical behavior of single-walled carbon nanotube/polypropylene/ethylene-propylene-diene rubber nanocomposites, *J Appl Polym Sci*, **89**, 2657-2663, 2003.
2. Kearns JC, Shambaugh RL, Polypropylene fibers reinforced with carbon nanotubes, *J Appl Polym Sci*, **86**, 2079-2084, 2002.
3. Du F, Scogna RC, Zhou W, Brand S, Fischer JE, Winey KI, Nanotube networks in polymer nanocomposites: rheology and electrical conductivity, *Macromolecules*, **37**, 9048-9055, 2004.
4. Eitan A, Fisher FT, Andrews R, Brinson LC, Schadler LS, Reinforcement mechanisms in MWCNT-filled polycarbonate, *Compos Sci Technol*, **66**, 1159-1170, 2006.
5. Ramanathan T, Liu H, Brinson LC, Functionalized SWNT/polymer nanocomposites for dramatic property improvement, *J Polym Sci B Polym Phys*, **43**, 2269-2279, 2005.
6. López-Manchado MA, Valentini L, Biagiotti J, Kenny JM, Thermal and mechanical properties of single-walled carbon nanotubes-polypropylene composites prepared by melt processing, *Carbon*, **43**, 1499-1505, 2005.
7. Funck A, Kaminsky W, Polypropylene carbon nanotube composites by in situ polymerization, *Compos Sci Technol*, **67**, 906-915, 2007.
8. Bhattacharyya AR, Pötschke P, Mechanical properties and morphology of melt-mixed PA6/SWNT composites: effect of reactive coupling, *Macromol Symp*, **233**, 161-169, 2006.
9. Pötschke P, Bhattacharyya AR, Janke A, Melt mixing of polycarbonate with multiwalled carbon nanotubes: microscopic studies on the state of dispersion, *Eur Polym J*, **40**, 137-148, 2004.
10. Pötschke P, Bhattacharyya AR, Janke A, Morphology and electrical resistivity of melt mixed blends of polyethylene and carbon nanotube filled polycarbonate, *Polymer*, **44**, 8061-8069, 2003.
11. Bhattacharyya AR, Pötschke P, Häußler L, Fischer D, Reactive compatibilization of melt mixed PA6/SWNT composites: mechanical properties and morphology, *Macromol Chem Phys*, **206**, 2084-2095, 2005.
12. Fisher FT, Bradshaw RD, Brinson LC, Effects of nanotube waviness on the modulus of nanotube-reinforced polymers, *Appl Phys Lett*, **80**, 4647-4649, 2002.
13. Wang B, Sun G, Liu J, He X, Li J, Crystallization behavior of carbon nanotubes-filled polyamide 1010, *J Appl Polym Sci*, **100**, 3794-3800, 2006.
14. Jin J, Song M, Pan F, A DSC study of effect of carbon nanotubes on crystallization behaviour of poly(ethylene oxide), *Thermochimica Acta*, **456**, 25-31, 2007.
15. Mitchel CA, Bahr JL, Arepalli S, Tour JM, Krishnamoorti R, Dispersion of functionalized carbon nanotubes in polystyrene, *Macromolecules*, **35**, 8825-8830, 2002.
16. Sandler J, Shaffer MSP, Prasse T, Bauhofer W, Schulte K, Windle AH, Development of a dispersion process for carbon nanotubes in an epoxy matrix and the resulting electrical properties, *Polymer*, **40**, 5967-5971, 1999.
17. Assouline E, Lustiger A, Barber AH, Cooper CA, Klein E, Wachtel E, Wagner HD, Nucleation ability of multiwall carbon nanotubes in polypropylene composites, *J Polym Sci B Polym Phys*, **41**, 520-527, 2003.
18. Valentini L, Biagiotti J, Kenny JM, Santucci S, Effects of single-walled carbon nanotubes on the crystallization behavior of polypropylene, *J Appl Polym Sci*, **87**, 708-713, 2003.
19. Xia HS, Wang Q, Li KS, Hu GJ, Preparation of polypropylene/carbon nanotube composite powder with a solid-state mechanochemical pulverization process, *J Appl Polym Sci*, **93**, 378-386, 2004.
20. Liu TX, Phang IY, Shen L, Chow SY, Zhang WD, Morphology and mechanical properties of multiwalled carbon nanotubes reinforced nylon-6 com-

posites, *Macromolecules*, **37**, 7214-7222, 2004.
21. Du F, Fischer JE, Winey KI, Coagulation method for preparing single-walled carbon nanotube/poly(methyl methacrylate) composites and their modulus, electrical conductivity, and thermal stability, *J Polym Sci B Polym Phys*, **41**, 3333-3338, 2003.
22. Di Lorenzo ML, Silvestre C, Non-isothermal crystallization of polymers, *Prog Polym Sci*, **24**, 917-950, 1999.
23. Bhattacharyya AR, Sreekumar TV, Liu T, Kumar S, Ericson LM, Hauge RH, Smalley RE, Crystallization and orientation studies in polypropylene/single wall carbon nanotube composite, *Polymer*, **44**, 2373-2377, 2003.
24. Grady BP, Pompeo F, Shambaugh RL, Resasco DE, Nucleation of polypropylene crystallization by single-walled carbon nanotubes, *J Phys Chem B*, **106**, 5852-5858, 2002.
25. Valentini L, Biagiotti J, López-Manchado MA, Santucci S, Kenny JM, Effects of carbon nanotubes on the crystallization behavior of polypropylene, *Polym Eng Sci*, **44**, 303-311, 2004.
26. Seo M-K, Lee J-R, Park S-J, Crystallization kinetics and interfacial behaviors of polypropylene composites reinforced with multi-walled carbon nanotubes, *Mater Sci Eng A*, **404**, 79-84, 2005.
27. Valentini L, Biagiotti J, Kenny JM, Santucci S, Morphological characterization of single-walled carbon nanotubes-PP composites, *Compos Sci Technol*, **63**, 1149-1153, 2003.
28. Leelapornpisit W, Ton-That M-T, Perrin-Sarazin F, Cole KC, Denault J, Simard B, Effect of carbon nanotubes on the crystallization and properties of polypropylene, *J Polym Sci B Polym Phys*, **43**, 2445-2453, 2005.
29. Yuan Q, Awate S, Misra RDK, Nonisothermal crystallization behavior of melt-intercalated polyethylene-clay nanocomposites, *J Appl Polym Sci*, **102**, 3809-3818, 2006.
30. Fillon B, Lotz B, Thierry A, Wittmann JC, Self-nucleation and enhanced nucleation of polymers. Definition of a convenient calorimetric "efficiency scale" and evaluation of nucleating additives in isotactic polypropylene (α phase), *J Polym Sci B Polym Phys*, **31**, 1395-1405, 1993.
31. Hay JN, Application of the modified Avrami equations to polymer crystallization kinetics, *Br Polym J*, **3**, 73-82, 1971.
32. Lu XF, Hay JN, Isothermal crystallization kinetics and melting behaviour of poly(ethylene terephthalate), *Polymer*, **42**, 9423-9431, 2001.
33. Hay JN, Fitzgerald PA, Wiles M, Use of differential scanning calorimetry to study polymer crystallization kinetics, *Polymer*, **17**, 1015-1018, 1976.
34. Hay JN, Sharma L, Crystallization of poly(3-hydroxybutyrate)/polyvinyl acetate blends, *Polymer*, **41**, 5749-5757, 2000.
35. Hay JN, Crystallization from the melt. In: *Flow-Induced Crystallization in Polymer Systems*, Miller RL (Ed), Gordon & Beach, UK, 72, 1979.
36. Jabarin SA, Crystallization kinetics of polyethylene terephthalate. II: dynamic crystallization of PET, *Appl Polym Sci*, **34**, 97-102, 1987.
37. Yu J, He J, Crystallization kinetics of maleic anhydride grafted polypropylene ionomers, *Polymer*, **41**, 891-898, 2000.
38. Razavi-Nouri M, Hay JN, Evaluation of the crystallization kinetics and melting of polypropylene and metallocene-prepared polyethylene blends, *J Appl Polym Sci*, **104**, 634-640, 2007.
39. Gao J, Wang D, Yu M, Yao Z, Nonisothermal crystallization, melting behavior, and morphology of polypropylene/metallocene-catalyzed polyethylene blends, *J Appl Polym Sci*, **93**, 1203-1210, 2004.
40. Jeziorny A, Parameters characterizing the kinetics of the non-isothermal crystallization of poly(ethylene terephthalate) determined by DSC, *Polymer*, **19**, 1142-1144, 1978.
41. Xu W, Liang G, Wang W, Tang S, He P, Pan W-P, Poly(propylene)-poly(propylene)-grafted maleic anhydride-organic montmorillonite (PP-PP-*g*-MAH-Org-MMT) nanocomposites. II: nonisothermal crystallization kinetics, *J Appl Polym Sci*, **88**, 3093-3099, 2003.
42. Liu S, Yu Y, Cui Y, Zhang H, Mo Z, Isothermal and nonisothermal crystallization kinetics of nylon-11, *J Appl Polym Sci*, **70**, 2371-2380, 1998.
43. Xu W, Ge M, He P, Nonisothermal crystallization

kinetics of polypropylene/montmorillonite nanocomposites, *J Polym Sci B Polym Phys*, **40**, 408-414, 2002.
44. Srinivas S, Babu JR, Riffle JS, Wilkes GL, Kinetics of isothermal and nonisothermal crystallization of novel poly(arylene ether ether sulfide)s, *Polym Eng Sci*, **37**, 497-510, 1997.
45. Ozawa T, Kinetics of non-isothermal crystallization, *Polymer*, **12**, 150-158, 1971.
46. An Y, Dong L, Mo Z, Liu T, Feng Z, Nonisothermal crystallization kinetics of poly(β-hydroxybutyrate), *J Polym Sci B Polym Phys*, **36**, 1305-1312, 1998.
47. Liu T, Mo Z, Wang S, Zhang H, Nonisothermal melt and cold crystallization kinetics of poly(aryl ether ether ketone ketone), *Polym Eng Sci*, **37**, 568-575, 1997.
48. Ziabicki A, Theoretical analysis of oriented and non-isothermal crystallization. II: extension of the Kolmogoroff-Avrami-Evans theory onto processes with variable rates and mechanisms, *Coll Polym Sci*, **252**, 433-447, 1974.
49. Supaphol P, Dangseeyun N, Srimoaon P, Nithitanakul M, Nonisothermal melt-crystallization kinetics for three linear aromatic polyesters, *Thermochimica Acta*, **406**, 207-220, 2003.
50. Chen M, Tian G, Zhang Y, Wan C, Zhang Y, Effect of silicon dioxide on crystallization and melting behavior of polypropylene, *J Appl Polym Sci*, **100**, 1889-1898, 2006.
51. Jang GS, Cho WJ, Ha CS, Crystallization behavior of polypropylene with or without sodium benzoate as a nucleating agent, *J Polym Sci B Polym Phys*, **39**, 1001-1016, 2001.
52. Wang J, Dou Q, Non-isothermal crystallization kinetics and morphology of isotactic polypropylene (iPP) nucleated with rosin-based nucleating agents, *J Macromol Sci B Phys*, **46**, 987-1001, 2007.
53. Hu X, Lesser AJ, Non-isothermal crystallization of poly(trimethylene terephthalate) (PTT)/clay nanocomposites, *Macromol Chem Phys*, **205**, 574-580, 2004.
54. Li J, Zhou CX, Wang G, Study on nonisothermal crystallization of maleic anhydride grafted polypropylene/montmorillonite nanocomposite, *Polym Test*, **22**, 217-223, 2003.
55. Hong P-D, Chung W-T, Hsu C-F, Crystallization kinetics and morphology of poly(trimethylene terephthalate), *Polymer*, **43**, 3335-3343, 2002.
56. Umemoto S, Hayashi R, Kawano R, Kikutani T, Okui N, Molecular weight dependence of primary nucleation rate of poly(ethylene succinate), *J Macromol Sci B Phys*, **B42**, 421-430, 2003.
57. Lauritzen JI, Hoffman JD, Extension of theory of growth of chain-folded polymer crystals to large undercoolings, *J Appl Phys*, **44**, 4340-4352, 1973.
58. Hoffman JD, The kinetic substrate length in nucleation-controlled crystallization in polyethylene fractions, *Polymer*, **26**, 803-810, 1985.
59. Hoffman JD, Theory of the substrate length in polymer crystallization: surface roughening as an inhibitor for substrate completion, *Polymer*, **26**, 1763-1778, 1985.
60. Hoffman JD, Miller RL, Test of the reptation concept: crystal growth rate as a function of molecular weight in polyethylene crystallized from the melt, *Macromolecules*, **21**, 3038-3051, 1988.
61. Hoffman JD, Miller RL, Response of criticism of nucleation theory as applied to crystallization of lamellar polymers, *Macromolecules*, **22**, 3502-3505, 1989.
62. Feng Y, Hay JN, The measurement of compositional heterogeneity in a propylene-ethylene block copolymer, *Polymer*, **39**, 6723-6731, 1998.
63. Li G, Yang S, Jiang J, Jin J, Wu C, The complicated influence of branching on crystallization behavior of poly(ethylene terephthalate), *J Appl Polym Sci*, **110**, 1649-1655, 2008.
64. Clark EJ, Hoffman JD, Regime III crystallization in polypropylene, *Macromolecules*, **17**, 878-885, 1984.
65. Nedkov E, Dobreva T, Kinetics of non-isothermal melting and crystallization of gamma-irradiated isotactic polypropylene, e-Polymers, No.**035**, 2003.
66. Zhou Z, Wang S, Lu L, Zhang Y, Zhang Y, Isothermal crystallization kinetics of polypropylene with silane functionalized multi-walled carbon nanotubes, *J Polym Sci B Polym Phys*, **45**, 1616-1624, 2007.